View metadata, citation and similar papers at core.ac.uk

brought to you by CORE

provided by Open Archive Toulouse Archive Ouverte

OATAO

Open Archive Toulouse Archive Ouverte

Open Archive Toulouse Archive Ouverte

OATAO is an open access repository that collects the work of Toulouse researchers and makes it freely available over the web where possible

This is an author's version published in: http://oatao.univ-toulouse.fr/24265

Official URL: https://doi.org/10.1016/j.electacta.2019.01.169

To cite this version:

Claquesin, Julien and Lemoine, Olivier and Gibilaro, Mathieu and Massot, Laurent and Chamelot, Pierre and Bourges, Gilles *Electrochemical behavior of plutonium fluoride species in LiF-CaF2 eutectic melt.* (2019) Electrochimica Acta, 301. 80-86. ISSN 0013-4686

Any correspondence concerning this service should be sent to the repository administrator: tech-oatao@listes-diff.inp-toulouse.fr

Electrochemical behavior of plutonium fluoride species in LiF-CaF_2 eutectic melt

Julien Claquesin [a, b], Olivier Lemoine [a], Mathieu Gibilaro [b, *], Laurent Massot [b], Pierre Chamelot [b], Gilles Bourges [a]

[a] CEA, DAM, VALDUC, F-21120, Is-sur-Tille, France
[b] Laboratoire de Génie Chimique UMR 5503 UPS-CNRS-INP, Université de Toulouse, 118 Route de Narbonne, F-31062, Toulouse, France

A B S T R A C T

The electrochemical behavior of plutonium fluoride species was investigated in molten LiF-CaF_2 medium in the 1093–1153 K temperature range with PuF_4 additions. A preliminary thermodynamic study supposed a Pu(IV) carboreduction into Pu(III) and that Pu(III) reduction into metal proceeds in one step. Then, an electrochemical study was carried out on an inert electrode (tungsten) and confirmed the thermodynamic predictions: Pu(IV) is spontaneously reduced into Pu(III) in presence of carbon and Pu(III) is directly reduced into Pu(0): $Pu(III) + 3e^- = Pu(0)$.

Moreover, Pu(III) reduction mechanism is a diffusion controlled process. Diffusion coefficients were calculated at different temperatures and obey to an Arrhenius' type law with an activation energy of 63 ± 3 kJ mol^{-1}. The standard potential of Pu(III)/Pu(0) was determined at 1113 K and is found to be −4.61 V vs. $F_{2\ (gaz)}/F^-$. This value permitted to calculate activity coefficients for several molalities.

Keywords:
Molten fluoride
Electrochemistry
Plutonium
Cyclic voltammetry
Chronopotentiometry

1. Introduction

Pyrochemical processes in molten salt media are considered as a promising option for future nuclear fuel cycle or for waste streams treatment containing actinides. Among the molten salts used as solvent for these processes, the chloride media were extensively studied for fuel reprocessing in several countries [1–3], and were also employed for defense applications programs.

Pyrochemical processing in molten fluoride media is investigated in the frame of future nuclear fuel cycle. For instance, the molten salt fast reactor option of Gen-IV international forum involves a mixture of LiF-ThF_4 (UF_4/UF_3) as nuclear fuel [4–6].

LiF-AlF_3 molten mixture was also investigated for the treatment of products containing minor actinides. The process involves the use of a liquid/liquid reductive extraction step where the fluoride salt, which contains the dissolved actinides, is contacted with liquid aluminum pool [7] in order to decontaminate the slag.

Another example is the preparation of metallic actinides, such as uranium or plutonium, performed in fluoride media via metallothermic reduction [8,9], where actinide fluoride is reduced into metal with metallic calcium such as:

$$2\ AnF_x + x\ Ca = x\ CaF_2 + 2\ An \quad (1)$$

The fluorite by-product (CaF_2) still contains actinides compounds (metal, fluoride, oxide, oxifluoride) and is then investigated by the CEA to be decontaminated by a similar process.

A good knowledge of the actinide behavior in the molten salt media is essential to operate these processes. Whatever the process route is, liquid/liquid extraction or metallothermic reduction, thermochemical data and electrochemical behavior allow determining the best conditions for process control: separation yield, impact of impurities such as oxides and, as a result, selective extraction of undesirable elements.

Among actinides, plutonium was chosen as element of study. In chloride media, electrochemical studies were carried out on $PuCl_3$ on inert electrode in LiCl-KCl by Serp et al. [10] and O. Shirai et al. [11,12]. They found that Pu(III) reduction proceeds via a one-step process with 3 electrons exchanged. The system is found to be quasi-reversible and diffusion controlled by both authors. Pu(III) diffusion coefficient was determined at 733 K by Serp, and the value is found to be 1.6×10^{-5} $cm^2\ s^{-1}$. Contrary to chloride media, very limited studies are available in fluoride media. Electrochemical study of PuF_3 in LiF-NaF-BeF_2 was performed at 893 K by Zakirov

* Corresponding author.
E-mail address: gibilaro@chimie.ups-tlse.fr (M. Gibilaro).

https://doi.org/10.1016/j.electacta.2019.01.169
0013-4686/

et al. [13]. Only one electrochemical system was detected and attributed to the Pu(III) reduction into Pu(0) at around 0.1 V from the Be(II) reduction (solvent reduction). PuF_3 behavior was also investigated by Hamel et al. [14] in LiF-CaF_2. However, because of oxide content pollution, the authors showed only the existence of several oxifluoride species. Due to the lack of data, it is of interest to lead a new and complete investigation in a fluoride media.

In this work, the electrochemical and chemical properties of plutonium fluoride were studied in LiF-CaF_2 eutectic mixture in the 1093–1153 K temperature range. Transient electrochemical techniques such as cyclic voltammetry, square wave voltammetry and chronopotentiometry were used to investigate the plutonium ions electrochemical reduction mechanism. Diffusion coefficient, standard potential of Pu(III)/Pu(0) system and activity coefficients of Pu(III) were determined.

2. Experimental

The cell consisted of a vitreous carbon crucible placed in a magnesia container, positioned in a cylindrical vessel made of refractory steel and closed with a stainless steel lid. The inner part of the walls was protected against fluoride vapours by a tantalum liner. The setup was located in a glove box kept under an inert argon atmosphere.

The electrolyte bath consisted of a eutectic LiF-CaF_2 mixture (Alfa Aesar 99.99% ampouled under argon) (79.2/20.8 M ratio), prepared by mixing the pure chemicals in the glove box. The salt was heated up to 1173 K at 1 K min^{-1} and kept at this temperature for 2 h to ensure a good homogeneity of the melt. Plutonium ions were introduced into the bath in the form of PuF_4 powder, synthesized by direct fluorination of PuO_2 previously purified by an internal hydrometallurgical process.

Tungsten wire (Alfa Aesar 99.95%, 1 mm diameter) was used as working electrode. Its surface was determined after each experiment by measuring the immersion depth in the bath. The auxiliary electrode was a vitreous carbon (V25) rod (3 mm diameter) with a large surface area ($\approx 1.5\ cm^2$).

The potentials were referred to a platinum wire (Alfa Aesar 99.95%, 1 mm diameter) immersed in the electrolyte acting as a quasi-reference electrode $Pt/PtO_x/O^{2-}$ according to Ref. [15].

The electrochemical study was performed using an Autolab PGSTAT302 N potentiostat/galvanostat controlled with GPES 4.9 software.

Cyclic voltammetry, square wave voltammetry and chronopotentiometry were used to investigate the electrochemical system.

3. Results and discussion

3.1. Preliminary discussions

The *E-pCaO* diagram shown in Fig. 1, also called potential-oxoacidity diagram, exhibits theoretical predominance domains of plutonium species in fluoride media at $T = 1113$ K using HSC 6.1 software. These domains are plotted on a potential scale vs. $F_{2\,(g)}/F^-$ and vary as a function of the oxide content defined by $pCaO = -\log(a_{CaO})$. Activities of soluble species (PuF_3 and PuF_4) were chosen equal to 0.1, and activity of LiF was considered identical to its molar ratio 0.792. The potential of LiF/Li is also displayed at −5.30 V vs. $F_{2\,(g)}/F^-$ which corresponds to the solvent reduction.

From this diagram, it can be predicted that for relatively high oxide content ($pCaO < 9$), stable plutonium species are PuO_2, PuOF and Pu whereas at lower oxide content ($pCaO > 9$), the stable species are PuF_4, PuF_3 and Pu. This indicates that oxide content in the bath must be kept as low as possible to have plutonium fluoride species in the salt.

According to this diagram, Pu(IV) reduction into Pu(0) should proceed through two electrochemical reactions:

$$Pu(IV) + 1e^- = Pu(III) \quad (2)$$

$$Pu(III) + 3e^- = Pu(0) \quad (3)$$

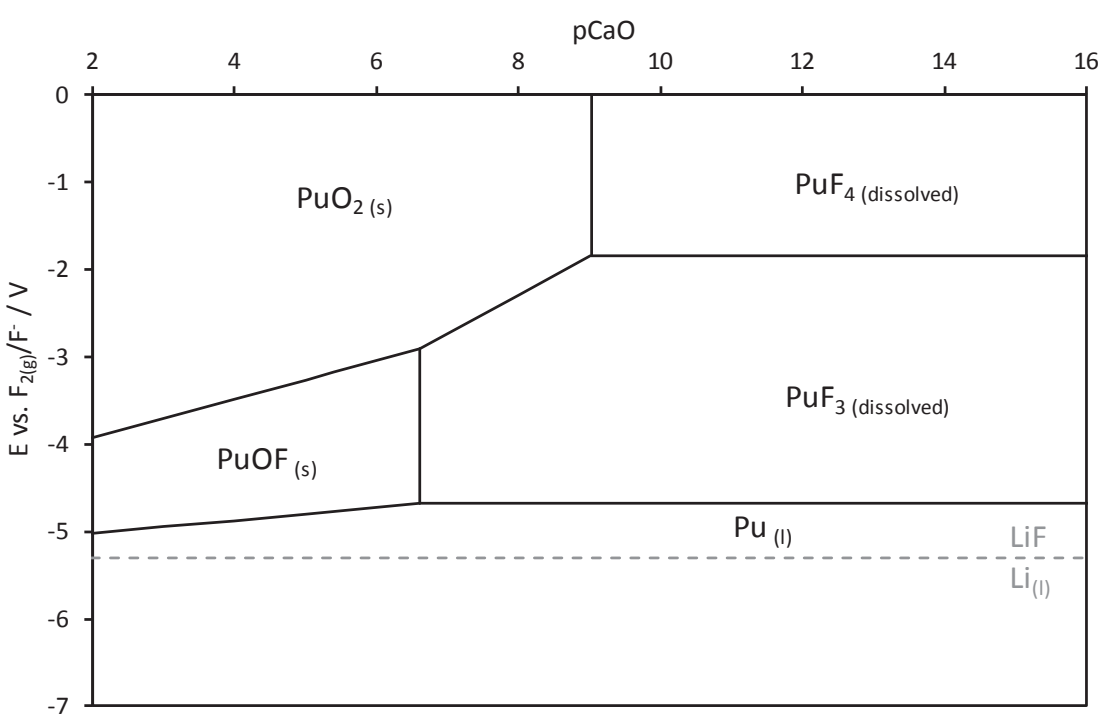

Fig. 1. Theoretical *E-pCaO* diagram of plutonium in LiF-CaF_2 eutectic system at $T = 1113$ K with activities of Pu(IV) and Pu(III) chosen equal to 0.1 using HSC 6.1.

The standard potentials of Pu(IV)/Pu(III) and Pu(III)/Pu(0) are respectively −1.84 V and −4.68 vs. $F_{2\,(g)}/F^-$. These reactions can be electrochemically studied since metal deposition takes place at 0.62 V from the solvent reduction potential.

Pu ions are introduced into the bath in the form of PuF_4. In presence of carbon constituting the crucible (CF_4/C), PuF_4 can be reduced:

$$4\ PuF_4 + C = 4\ PuF_3 + CF_{4\ (gas)} \tag{4}$$

The Gibbs energy associated to reaction (4) at 1113 K using HSC 6.1 software is −54.209 kJ mol^{-1}, which indicates that PuF_4 carboreduction is spontaneous: only Pu(III) should exist in the bath. Starting from PuF_3 in the molten solvent and according to the theoretical thermodynamic diagram (Fig. 1), the electrochemical reduction of Pu(III) into Pu(0) is expected to be a one-step process with an exchange of 3 electrons, following the reaction (3).

3.2. Reduction mechanism of plutonium fluoride on inert electrode

3.2.1. Confirmation of the thermodynamic predictions

Square wave voltammetry was used to verify the previous thermodynamic study. This method consists in a potential scanning proceeding stepwise with superimposition on each step of the staircase of two potentials pulses, direct and reverse, of the same intensity. Plotting the differential current measured at each step between the successive pulses as a function of the potential associated to each electrochemical reaction, a Gaussian shaped peak is obtained. When the product is a soluble compound, the number of exchanged electrons can be calculated using the following relationship [16–19]:

$$W_{1/2} = 3.52\frac{RT}{nF} \tag{5}$$

where $W_{1/2}$ is the half-width of the peak (V), R the ideal gas constant (J mol^{-1} K^{-1}), T the temperature (K), n the number of exchanged electrons and F the Faraday constant (C mol^{-1}).

Fig. 2 presents a square wave voltammogram performed in LiF-CaF_2 on tungsten electrode at 16 Hz and T = 1113 K after PuF_4 addition (0.086 mol kg^{-1}). A single peak is observed at around −1 V vs. Pt prior the solvent reduction Li(I) at around −1.3 V vs. Pt, corresponding to the cathodic limit. The shape is a Bigaussian type, caused by a nucleation overvoltage, characteristic of an insoluble phase reduction on the working electrode, confirming the Pu(0) formation. The validity of equation (5) is verified in the frequency range 9–51 Hz by the linear relationship between the peak current density versus the square root of the frequency (Fig. 2 inset). Furthermore, the reduction peak potential is independent of the frequency which indicates that the reaction is quasi-reversible. In this case, the method to determine the half-width of the peak ($W_{1/2}$) is described in Ref. [20]. The signal is deconvoluted using OriginPro software (2016) to obtain an accurate value of W_L and then $W_{1/2} = 2 \times W_L$. The number of exchanged electrons is found to be 3.0 ± 0.1. The nucleation overvoltage was also evaluated as described in Ref. [21], and the obtained value is 37 ± 3 mV.

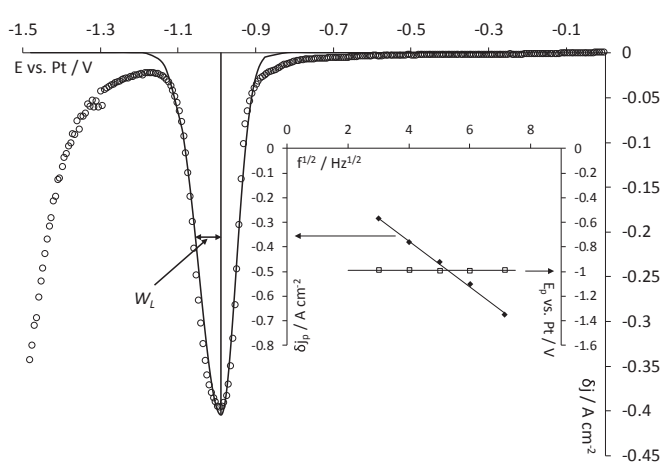

Fig. 2. Square wave voltammogram on W in LiF-CaF_2 eutectic melt after PuF_4 addition (0.086 mol kg^{-1}) at 16 Hz and T = 1113 K. Working el.: W (S ≈ 0.25 cm^2); auxiliary el.: vitreous carbon; comparison el.: Pt. Inset. variation of the peak current density (left axis) and the reduction peak potential (right axis) vs. the square root of frequency.

Since Pu(0) is deposited with exchange of 3 electrons on the working electrode, the only possible precursor in molten fluoride without oxide is Pu(III) in agreement with the theoretical calculations. As reaction (4) is equimolar regarding the plutonium species, PuF_4 additions lead to the same PuF_3 concentration.

Then, a cyclic voltammetry was performed on an inert tungsten electrode. A typical voltammogram in LiF-CaF_2 at T = 1113 K and 100 mV s^{-1} is shown in Fig. 3. The cathodic and anodic limits correspond respectively to the solvent reduction (Li(I)), as it was previously observed in Fig. 2, and to the oxidation of the working electrode material (W). Only one redox system is observed at around 0.55 V before the solvent reduction confirming the previous results. This value is similar to the one previously calculated for the Pu(III)/Pu(0) system.

A single peak (I_C) is observed in the cathodic run at around −1.03 V vs. Pt, associated to an anodic peak (I_A) at around −0.88 V vs. Pt exhibiting an abrupt decrease of the current density. This shape is typical of a solid phase reoxidation on the working electrode (stripping peak). Furthermore, the cathodic peak current density increases linearly with the Pu(III) content at a given temperature, as it is shown in Fig. 4. The slope of the calibration curve is found to be −3.02 ± 0.07 A kg cm^{-2} mol^{-1} and can be used to determine the Pu(III) concentration into the bath.

To confirm Pu deposition on the working electrode surface, a reversal chronopotentiogram was carried out at ±100 mA and T = 1113 K (m_0 = 0.086 mol kg^{-1}) and the signal is plotted in Fig. 5. The anodic transition time τ_{reox} is found to be equal to the cathodic one with $\tau_{reox} = \tau_{red}$ = 0.54 s and is typical of a solid phase deposition on the working electrode [22]. This observation is in agreement with the previous results showing that Pu(III) is reduced in Pu(0) via a one-step process and are consistent with the ones obtained by Zakirov in LiF-NaF-BeF_2 medium [13].

3.2.2. Pu(III) reduction limiting process

To investigate the Pu(III) reduction limiting process, the cyclic voltammetry technique was used by plotting the scan rate influence on the peak current density (I_C) in Fig. 6. The current density increases linearly with the square root of the scan rate, which means that the electrochemical reduction of Pu(III) is controlled by a diffusion process. Thus, the Berzins-Delahay relationship was used for a reversible soluble/insoluble system, defined as follows [23]:

$$\frac{j_p}{\sqrt{v}} = 0.61\ (nF)^{3/2}(RT)^{-1/2}D^{1/2}C_0 = constant \tag{6}$$

where j_p is the peak current density (A cm^{-2}), v the potential scan rate (V s^{-1}), D the diffusion coefficient (cm^2 s^{-1}) and C_0 the solute concentration (mol cm^{-3}). The value obtained with the experimental data plotted in Fig. 6 is:

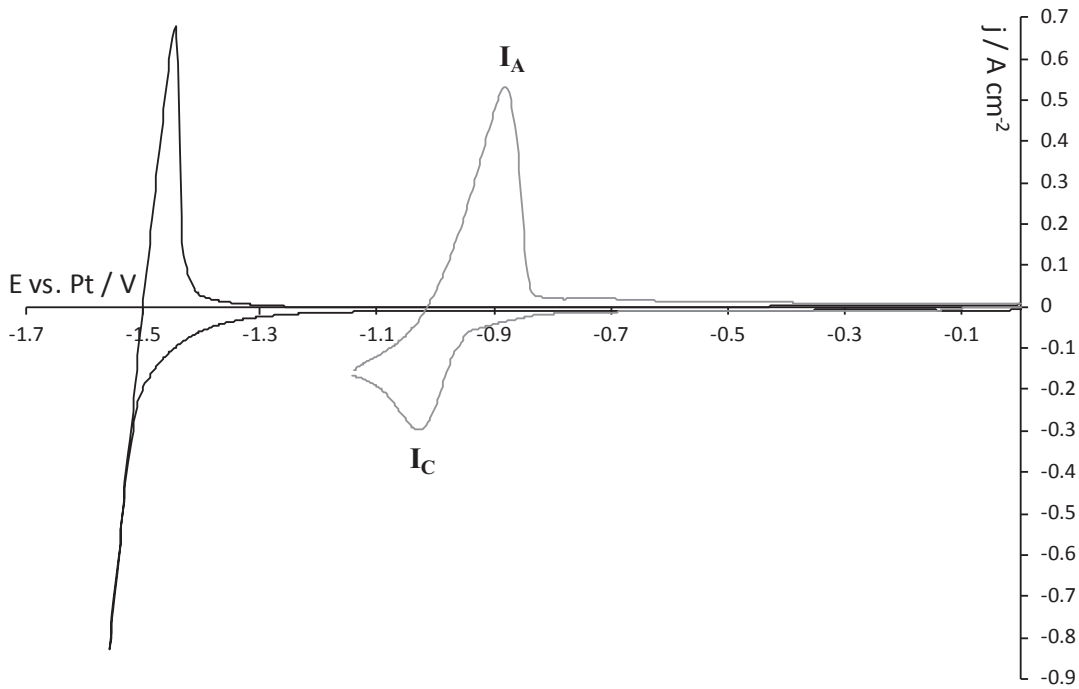

Fig. 3. Cyclic voltammograms on W of the eutectic LiF-CaF_2 system at 100 mV s^{-1} and T = 1113 K: pure solvent (black) and with Pu(III) concentration of 0.086 mol kg^{-1} (grey).

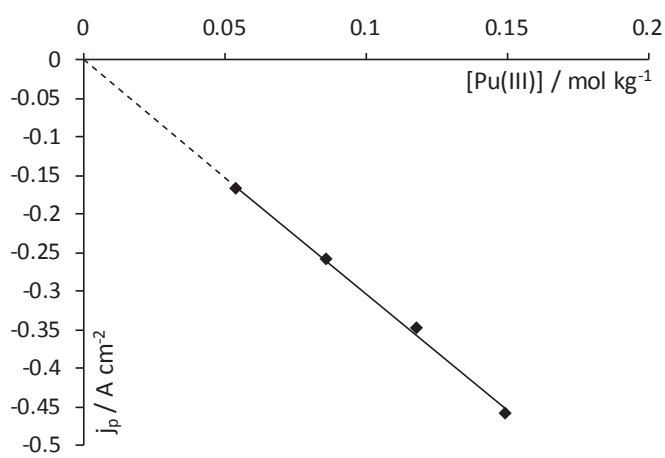

Fig. 4. Linear relationship between the cathodic peak current density and the Pu(III) content in the LiF-CaF_2 eutectic melt on inert electrode (W) at 1113 K and 100 mV s^{-1}.

$$\frac{j_p}{\sqrt{\nu}} = 0.98 \pm 0.01 \text{ A s}^{1/2} \text{ V}^{-1/2} \text{ cm}^{-2} \quad (7)$$

at $T = 1113$ K and $m_0 = 0.086$ mol kg^{-1}.

In order to confirm that the electrochemical reduction is a diffusion controlled process, chronopotentiometry was carried out on W from −60 mA to −160 mA at $T = 1093$ K ($m_0 = 0.086$ mol kg^{-1}). Chronopotentiograms are plotted in Fig. 7 and exhibit a single plateau at about −0.95 V vs. Pt, corresponding to the reduction potential of Pu(III) observed by cyclic voltammetry. It can be noticed that the transition time τ decreases when the applied current density increases. This observation is in agreement with the Sand's law [24]:

$$j\sqrt{\tau} = 0.5\, nFC_0\sqrt{\pi D} = constant \quad (8)$$

where τ is the transition time (s).

According to the data plotted in Fig. 7 inset, it gives:

$$j\sqrt{\tau} = -0.239 \pm 0.002 \text{ A s}^{1/2} \text{ cm}^{-2} \quad (9)$$

The Sand's law verification permits to confirm that the electrochemical reaction is effectively controlled by Pu(III) diffusion in the melt in agreement with chloride media studies [10–12].

3.3. Determination of experimental physico-chemical data

3.3.1. Diffusion coefficient determination

Diffusion coefficients (D) were calculated in the 1093–1153 K temperature range, using equation (6). For instance, at $T = 1113$ K and $m_0 = 0.086$ mol kg^{-1}, the diffusion coefficient is found to be $3.3 \pm 0.1 \times 10^{-5}$ cm^2 s^{-1}. In comparison with cerium which is usually used to simulate plutonium because of its similar physico-chemical properties (melting point, conductivity, redox potential, oxidation number …) [25], the Ce(III) diffusion coefficient determined by Gibilaro et al. [26] in LiF-CaF_2 melt at 1113 K is $2.64 \pm 0.43 \times 10^{-5}$ cm^2 s^{-1} and is in the same order of magnitude than the Pu(III) one. The linear relationship between ln D and the inverse absolute temperature, plotted in Fig. 8, demonstrates that the variation of the diffusion coefficient obeys to an Arrhenius' type law:

$$\ln D = -3.5\ (\pm 0.3) - \frac{7600\ (\pm 300)}{T} \quad (10)$$

From this relation, the activation energy was calculated and is found to be 63 ± 3 kJ mol^{-1} which is in agreement with cerium system in comparable conditions: 50 ± 2 kJ mol^{-1}.

3.3.2. Standard potential and activity coefficients determination

Thermodynamics data such as standard potential and activity coefficients of the Pu(III)/Pu(0) system were calculated at 1113 K according to the method described in Ref. [21]. First, the Pu(III)/Pu(0) standard potential $E^{\circ}_{Pu(III)/Pu(0)}$ was determined using Nernst equation:

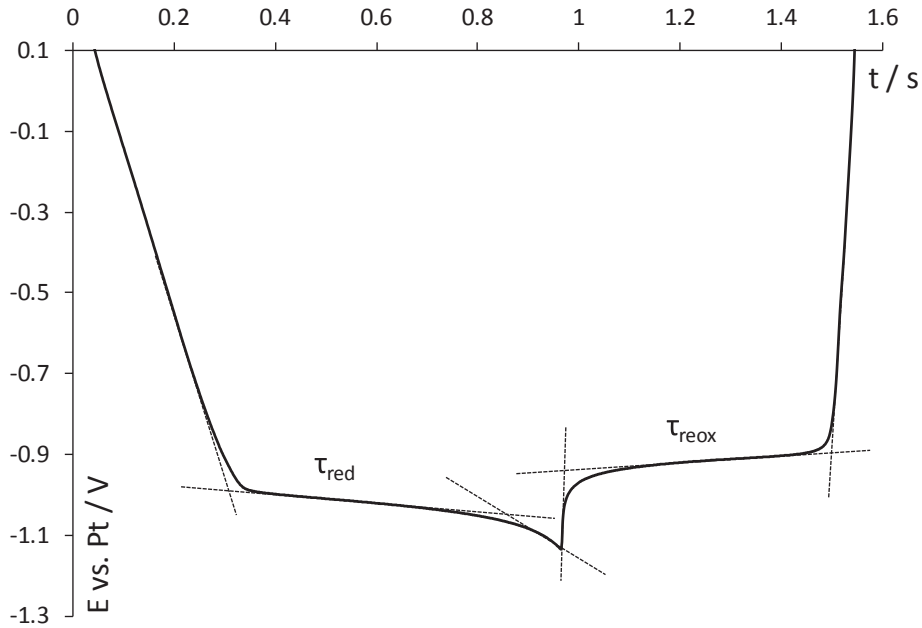

Fig. 5. Reversal chronopotentiogram on W of the LiF-CaF_2-Pu(III) system (0.086 mol kg^{-1}) at T = 1113 K; applied current = ±100 mA. Working El.: W (S ≈ 0.25 cm^2); auxiliary el.: vitreous carbon; comparison el.: Pt.

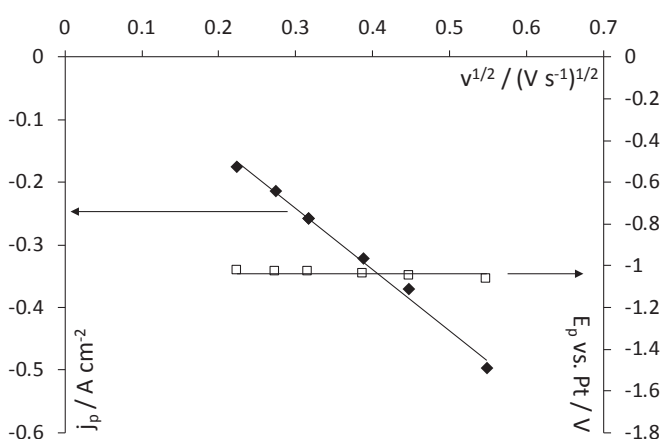

Fig. 6. Variation of the peak current density (left axis) and the reduction peak potential (right axis) vs. the square root of the potential scan rate on W in LiF-CaF_2-Pu(III) system (0.086 mol kg^{-1}) at T = 1113 K. Working el.: W (S ≈ 0.25 cm^2); auxiliary el.: vitreous carbon; comparison el.: Pt.

$$E_{Pu(III)/Pu(0)} = E^{\circ}_{Pu(III)/Pu(0)} + \frac{RT}{3F}\ln \gamma_{Pu(III)} + \frac{RT}{3F}\ln m_{Pu(III)} \quad (11)$$

where $E_{Pu(III)/Pu(0)}$ is the Pu(III)/Pu(0) experimental potential, $\gamma_{Pu(III)}$ the Pu(III) activity coefficient and $m_{Pu(III)}$ the Pu(III) molality. Equation (11) can also be written as $E_{Pu(III)/Pu(0)} - (RT/3F)\ln m_{Pu(III)} = E^{\circ}{}_{Pu(III)/Pu(0)} + (RT/3F)\ln \gamma_{Pu(III)}$, and the experimental values of $(E_{Pu(III)/Pu(0)} - (RT/3F)\ln m_{Pu(III)})$ were plotted as a function of the molality in Fig. 9.

Values of $E_{Pu(III)/Pu(0)}$ (vs. Pt) can be converted into $E_{Pu(III)/Pu(0)}$ (vs. $F_{2\ (g)}/F^-$) with internal reference methodology using Li(I)/Li (0) intermediate potential:

$$E_{Pu(III)/Pu(0)}\left(\text{vs. } F_{2\ (g)}/F^-\right) = \left[E_{Pu(III)/Pu(0)}\ (\text{vs. Pt}) + \eta\right] - E_{Li(I)/Li(0)}\ (\text{vs. Pt}) + E_{Li(I)/Li(0)}\ (\text{vs. } F_{2(g)}/F^-)$$

Where $E_{Pu(III)/Pu(0)}$ (vs. Pt) and $E_{Li(I)/Li(0)}$ (vs. Pt) were graphically determined by cyclic voltammetry (V), η is the nucleation overvoltage previously determined (V) and $E_{Li(I)/Li(0)}$ (vs. $F_{2\ (g)}/F^-$) is the calculated Li(I)/Li (0) potential referenced to the $F_{2\ (g)}/F^-$ system (cf. § 3.1) (V).

$E^{\circ}{}_{Pu(III)/Pu(0)}$ was determined by extrapolating the straight line toward 0 mol kg^{-1}, and therefore at infinite dilution ($\gamma_{Pu(III)} = 1$): the value of $E^{\circ}{}_{Pu(III)/Pu(0)}$ is found to be −4.61 V vs. $F_{2\ (g)}/F^-$. Afterward, activity coefficients were calculated. Results are shown in Fig. 8 and exhibit a decrease of γ when the molality increases, which is in good agreement with infinite dilution theory. According to these results, Pu(III) behaviors deviate from ideality when the concentration increases.

4. Conclusions

Electrochemical behavior of plutonium fluoride was investigated in LiF-CaF_2 eutectics on inert electrode (W). It was shown that Pu(IV) is spontaneously reduced into Pu(III) by carbon constituting the crucible. In our experimental conditions, only Pu(III) is stable in the bath. It was demonstrated that Pu(III) reduction is a one-step process exchanging three electrons:

$$Pu(III) + 3e^- = Pu(0)$$

The electrochemical reaction is controlled by the Pu ions diffusion in the molten salt and occurs at around 0.55 V from the Li(I) reduction. The diffusion coefficients of Pu(III) were calculated in the 1093–1153 K temperature range and obey to an Arrhenius' type law according to:

$$\ln D = -3.5\ (\pm 0.3) - \frac{7600\ (\pm 300)}{T}$$

Experimental Pu(III)/Pu(0) standard potential was determined at 1113 K and is found to be −4.61 V vs. $F_{2\ (g)}/F^-$. Using Nernst equation, activity coefficients were calculated at the same temperature, exhibiting a decrease when the molality increases.

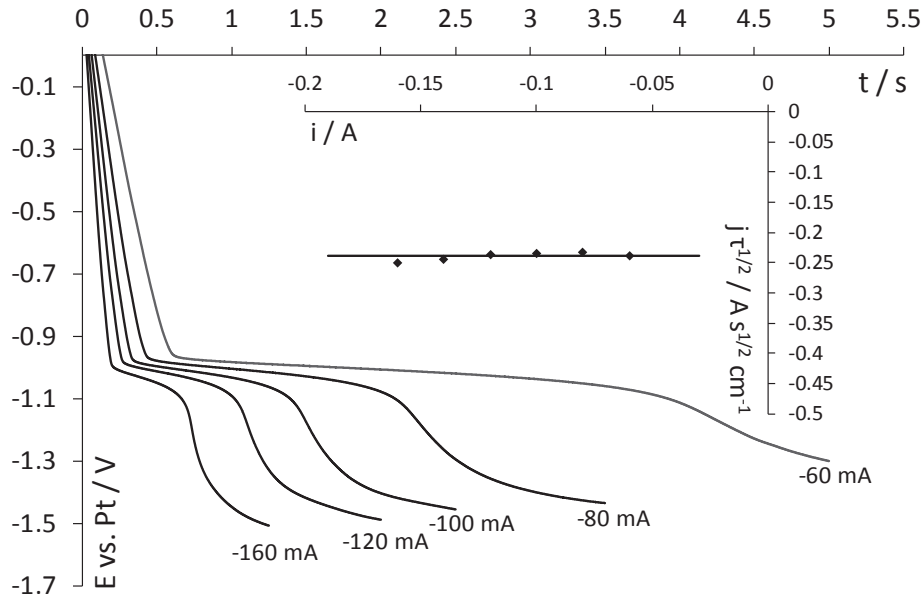

Fig. 7. Chronopotentiograms on W of the LiF-CaF_2-Pu(III) system (0.086 mol kg^{-1}) from −60 mA to −160 mA and T = 1093 K. Working El.: W (S ≈ 0.44 cm^2); auxiliary el.: vitreous carbon; comparison el.: Pt. Inset. variation of $i\tau^{1/2}$ vs. the intensity at 1093 K. Working el.: W (S ≈ 0.44 cm^2); auxiliary el.: vitreous carbon; comparison el.: Pt.

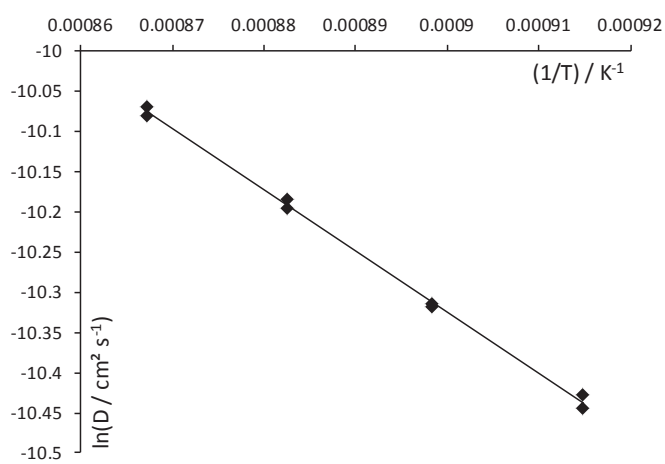

Fig. 8. Variation of the logarithm of the diffusion coefficient versus the inverse of the absolute temperature.

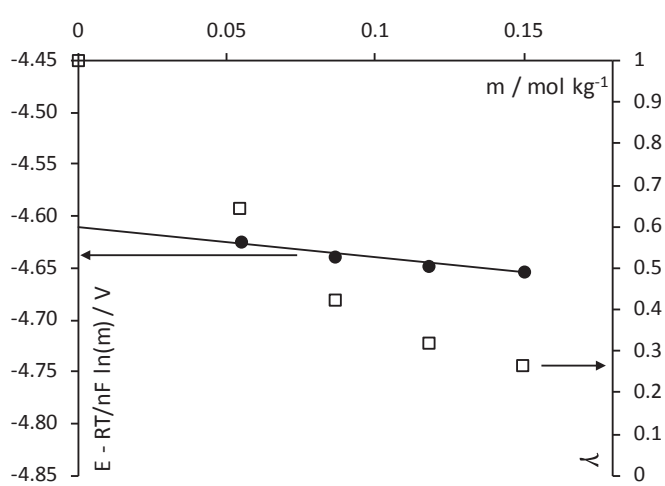

Fig. 9. Relationship between E − (RT/3 F) ln m (left axis) and activity coefficients (right axis) versus the molality m at 1113 K.

References

[1] J.J. Laidler, J.E. Battles, W.E. Miller, J.P. Ackerman, E.L. Carls, Development of pyroprocessing technology, Prog. Nucl. Energy 31 (1–2) (1997) 131.

[2] J.H. Ku, S.I. Moon, I.J. Cho, W.M. Choung, G.S. You, H.D. Kim, Development of pyroprocess integrated inactive demonstration facility, Procedia Chem 7 (2012) 779.

[3] T. Koyama, Y. Sakamura, M. Iizuka, T. Kayo, T. Murakami, J.-P. Glatz, Development of pyro-processing fuel cycle technology for closing actinide cycle, Procedia Chemistry 7 (2012) 772.

[4] D. Heuer, E. Merle-Lucotte, M. Allibert, M. Brovchenko, V. Ghetta, P. Rubiolo, Towards the thorium fuel cycle with molten salt fast reactors, Ann. Nucl. Energy 64 (2014) 421.

[5] P. Chamelot, L. Massot, L. Cassayre, P. Taxil, Electrochemical behaviour of thorium(IV) in molten LiF-CaF2 medium on inert and reactive electrodes, Electrochim. Acta 55 (16) (2010) 4758.

[6] C. Nourry, P. Soucek, L. Massot, R. Malmbeck, P. Chamelot, J.-P. Glatz, Electrochemistry of uranium in molten LiF-CaF2, J. Nucl. Mater. 430 (1–3) (2012) 58.

[7] E. Mendes, O. Conocar, A. Laplace, N. Douyère, M. Miguirditchian, Assessment of the complete core of the reference pyrochemical process, developed by the CEA, Procedia Chem 7 (2012) 791.

[8] R.D. Baker, B.R. Hayward, C. Hull, H. Raich, A.R. Weiss, Preparation of Uranium Metal by the Bomb Method, Los Alamos Scientific Lab., 1946. LA-472.

[9] R.D. Baker, Preparation of plutonium metal by the bomb method, Los Alamos Scientific Lab., 1946. LA-473.

[10] J. Serp, R.J.M. Konings, R. Malmbeck, J. Rebizant, C. Scheppler, J.-P. Glatz, Electrochemical behaviour of plutonium ion in LiCl-KCl eutectic melts, J. Electroanal. Chem. 561 (2004) 143.

[11] O. Shirai, T. Iwai, Y. Suzuki, Y. Sakamura, H. Tanaka, Electrochemical behavior of actinide ions in LiCl-KCl eutectic melts, J. Alloy. Comp. 271–273 (1998) 685.

[12] O. Shirai, M. Iizuka, T. Iwai, Y. Arai, Electrode reaction of Pu3+/Pu couple in LiCl-KCl eutectic melts: comparison of the electrode reaction at the surface of liquid Bi with that at a solid Mo electrode, Anal. Sci. 17 (2001) 51.

[13] R. Zakirov, V. Ignatiev, V. Subbotin, A. Toropov, Electrochemical properties of zirconium, plutonium and lanthanides in fluoride melts, in: Atalante 2004 Conference, Nîmes, France, 2004.

[14] C. Hamel, Séparation actinides-lanthanides (neodyme) par extraction électrolytique en milieux fluorures fondus, vol. 3, 2005. Thesis, Toulouse.

[15] Y. Berghoute, A. Salmi, F. Lantelme, Internal reference systems for fused electrolytes, J. Electroanal. Chem. 365 (1994) 171.

[16] L. Ramaley, M.S. Krause, Theory of square wave voltammetry, Anal. Chem. 41 (1969) 1362.

[17] M.S. Krause, L. Ramaley, Analytical application of square wave voltammetry, Anal. Chem. 41 (1969) 1365.

[18] J.G. Osteryoung, J.J. O'Dea, Square wave voltammetry, Electroanal. Chem. 14 (1986) 209.

[19] P. Chamelot, B. Lafage, P. Taxil, Using square-wave voltammetry to monitor molten alkaline fluoride baths for electrodeposition of niobium, Electrochim. Acta 43 (5–6) (1997) 607.

[20] C. Hamel, P. Chamelot, P. Taxil, Neodymiun(III) cathodic processes in molten

fluorides, Electrochim. Acta 49 (2004) 4467.
[21] C. Nourry, L. Massot, P. Chamelot, P. Taxil, Data acquisition in thermodynamic and electrochemical reduction in a Gd(III)/Gd system in LiF-CaF2 media, Electrochim. Acta 53 (2008) 2650.
[22] H.B. Herman, A.J. Bard, Diffusion controlled electrode reaction of a single component system, J. Anal. Chem. 35 (1963) 1121.
[23] A.J. Bard, L.R. Faulkner, Electrochemistry: Principles, Methods and Applications, Wiley Ed, New York, 1980.
[24] R.K. Jain, H.C. Gaur, B.J. Welch, Chronopotentiometry: a review of theoretical principles, J. Electroanal. Chem. 79 (1977) 211.
[25] B. Claux, Etude de la réduction électrochimique d'oxydes d'actinides en milieu de sels fondus, PhD thesis, Université Grenoble Alpes, Grenoble, 2011. in french.
[26] M. Gibilaro, Co-réduction électrochimique de l'aluminium et des lanthanides en milieu fluorures fondus, PhD thesis, Université Paul Sabatier, Toulouse, 2008. in french.